# Shear Stresses in Prismatic Beams with Arbitrary Cross–Sections

F. Gruttmann*, R. Sauer**, W. Wagner**

* *Institut für Statik, Technische Universität Darmstadt, Alexanderstraße 7, 64283 Darmstadt, Germany*

** *Institut für Baustatik, Universität Karlsruhe (TH), Kaiserstraße 12, D–76131 Karlsruhe, Germany*

**Abstract** In this paper the approximate computation of shear stresses in prismatic beams due to Saint–Venant torsion and bending using the finite element method is investigated. The shape of the considered cross–sections may be arbitrary. Furthermore the basic coordinate system lies arbitrarily to the centroid, and not necessarily in principal directions. For numerical reasons Dirichlet boundary conditions of the flexure problem are transformed into Neumann boundary conditions introducing a conjugate stress function. Based on the weak formulation of the boundary value problem isoparametric finite elements are formulated. The developed procedure yields the relevant warping and torsion constants.

# 1 Introduction

## 1.1 Motivation

The problem of torsional and flexural shearing stresses in prismatic beams has been discussed theoretically in several papers. Here, publications in [1,2,4,5] are mentioned among others. The problem of the center of shear and of twist has been studied in e.g. [4–8]. Furthermore, the text books of e.g. Timoshenko and Goodier [9] or Sokolnikoff [10] give detailed representations of the topics.
Numerical analysis of the torsion problem using the finite element method has been published e.g. in the following papers. Herrmann [12] applies the principle of minimum potential energy as basis for the development of finite elements. Anisotropic material behaviour has been incorporated by Krahula et al. [13] and Haberl et al. [14]. In [11–14] triangular and quadrilateral finite elements are used. Based on mixed variational principles warping functions and deformations of beam cross–sections are computed in Zeller [15,16]. Mason and Herrmann [11] introduce a displacement field for a beam subjected to bending. Based on this assumption the strains and stresses are evaluated by exploitation of the principle of minimum potential energy.
The goal of this paper is the computation of shear stresses due to torsion and bending in prismatic beams with arbitrary cross-sections using the finite element method. The essential features and novel aspects of the present formulation are summarized as follows.

(i) All basic equations are formulated with respect to an arbitrary Cartesian coordinate system which is not restricted to principal axes. Thus, the origin of this system is not necessarily a special point like the centroid. This relieves the input of the finite element data.

(ii) The boundary value problem of the Saint–Venant torsion is summarized. Especially for cross–sections with holes it turns out, that the formulation in terms of the warping function is better suitable for a finite element implementation than with



Published in: Int. J. Num. Meth. Engng., 45 (1999), 865-889.

Prandtl's stress function. The presented weak formulation and associated finite element implementation in terms of the warping function seem to be simpler than the versions in above discussed papers [12–16]. The developed procedure yields the relevant torsion and warping constants for arbitrary cross–sections.

(iii) The boundary value problem of a prismatic beam subjected to bending is described. A stress function is introduced which fulfills the equilibrium equations. Hence, reformulation of the Beltrami compatibility equations with the stress function yields the basic differential equation. The derived Dirichlet boundary conditions are difficult to implement in a finite element program. Therefore, an additional transformation is introduced which leads to a Neumann problem. The associated weak formulation is better suitable for a numerical implementation. The relationship to the proposed stress functions of Weber [1], Schwalbe [3] and Trefftz [4] is dicussed in section 4.1. The theory is different from above mentioned papers like [11, 15, 16] where all equations are based on a hypothesis for the displacement field. An alternative representation for two integration constants first given by Trefftz [4] is derived where the evaluation of Prandtl's stress function can be avoided.

(iv) The associated finite element formulation is based on isoparametric element functions. The resulting stiffness matrices and load vectors are easy to implement in a standard finite element program. We use the Zienkiewicz–Zhu criterion to steer an adaptive mesh refinement.

A brief summary of the paper is as follows. The shear stresses and section quantities for the pure torsion case are summarized in the next section. In section 3 torsionless bending of the rod is considered. The derived boundary value problem is split into two parts. It is shown, that the coordinates of the center of shear and of twist are identical. In section 4 finite element matrices based on the derived weak formulations of the torsion and bending problem are presented. We investigate several examples with various shapes of cross–section in section 5.

## 1.2 Basic equations

We consider a prismatic beam with arbitrary reference axis $x$ and section coordinates $y$ and $z$. The parallel system $\bar{y}$ and $\bar{z}$ intersects at the centroid with coordinates $\{y_S, z_S\}$, however not necessarily in principal directions. According to Fig. 1 the cross–section is denoted by $\Omega$ and the boundary by $\partial\Omega$. For some section quantities we use the notation $A_{ab} = \int_{(\Omega)} ab \, \mathrm{d}A$ and $A$ describes the area of the considered cross–section. The tangent vector $\mathbf{t}$ with associated coordinate $s$ and the outward normal vector $\mathbf{n} = [n_y, n_z]^T$ form a right–handed system. Thus, the direction of $s$ is defined in a unique way.
In the following two sections the vector of shear stresses $\boldsymbol{\tau} = [\tau_{xy}, \tau_{xz}]^T$ due to the loading cases torsion and bending is derived from the theory of linear elasticity. Thus, for further reference we summarize some basic equations. The equations of equilibrium neglecting volume forces read

$$\begin{aligned} \sigma_{x,x} + \tau_{xy,y} + \tau_{xz,z} &= 0 \\ \sigma_{y,y} + \tau_{yz,z} + \tau_{xy,x} &= 0 \\ \sigma_{z,z} + \tau_{xz,x} + \tau_{yz,y} &= 0\,, \end{aligned} \tag{1}$$

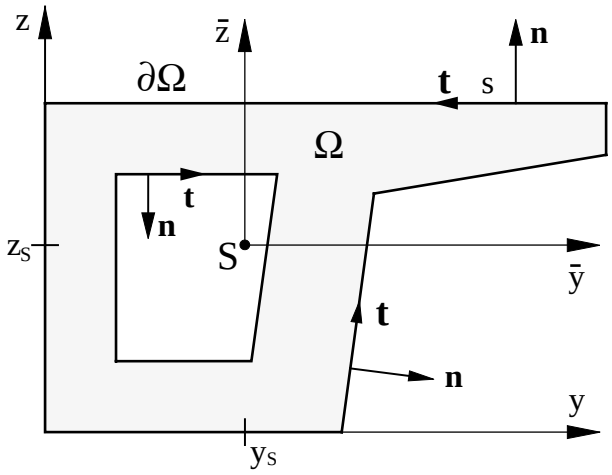


**Figure** 1: Cross–section $\Omega$ with outward normal vector

where commas denote partial differentiation. It is assumed that for prismatic beams the stress components $\sigma_y, \sigma_z, \tau_{yz}$ vanish. From $(1)_2$ and $(1)_3$ one concludes that the transverse shear stresses $\tau_{xy}$ and $\tau_{xz}$ cannot depend on $x$. As a consequence in the flexure case the shear forces $Q_y$ and $Q_z$ may not depend on $x$. Otherwise there is a contradiction to equilibrium equations (1). The rod is stress free along the cylindrical surface. Therefore, along the boundary of the cross–section the condition

$$\tau_{xy}\,\mathrm{d}z - \tau_{xz}\,\mathrm{d}y = 0 \qquad \text{on} \quad \partial\Omega \tag{2}$$

with $\mathrm{d}z = n_y \mathrm{d}s$ and $\mathrm{d}y = -n_z \mathrm{d}s$ must hold. This condition is visualized with the plots of the resulting shear stresses in section 5.
The strain–displacement relations are obtained by partial derivatives of the displacement field $\mathbf{u} = [u_x, u_y, u_z]^T$

$$\varepsilon_x = u_{x,x} \qquad \gamma_{xy} = u_{x,y} + u_{y,x} \qquad \gamma_{xz} = u_{x,z} + u_{z,x}\ . \tag{3}$$

Assuming linear elastic material behaviour, the stress strain relations read

$$\sigma_x = E\,\varepsilon_x \qquad \tau_{xy} = G\,\gamma_{xy} \qquad \tau_{xz} = G\,\gamma_{xz}\,, \tag{4}$$

where $E$ and $G$ denote Young's modulus and shear modulus, respectively.
Finally, the stress resultants are defined as follows

$$\begin{aligned} N &= \int_{(\Omega)} \sigma_x \,\mathrm{d}A & M_x &= \int_{(\Omega)} (\tau_{xz} y - \tau_{xy} z)\,\mathrm{d}A \\ Q_y &= \int_{(\Omega)} \tau_{xy}\,\mathrm{d}A & M_y &= \int_{(\Omega)} \sigma_x z\,\mathrm{d}A \\ Q_z &= \int_{(\Omega)} \tau_{xz}\,\mathrm{d}A & M_z &= -\int_{(\Omega)} \sigma_x y\,\mathrm{d}A\,. \end{aligned} \tag{5}$$

Here, $N, Q_y, Q_z$ denote the normal force and shear forces whereas $M_x, M_y, M_z$ denote the bending moments about the corresponding axes.

# 2 Saint–Venant torsion

In this section we summarize the basic equations of the torsion problem for prismatic beams for further reference. More detailed representations may be found in text books like e.g. [9,10]. In many practical applications with thin–walled cross–sections often a constant warping function can be assumed in thickness direction, e.g. see Bornscheuer [17]. Multicellular sections are cut to get open cross–sections. Hence, in each cell a constant circulating stress flux has to be superposed onto the solution of the open cross–section to obtain continuity at the interfaces. In this formulation the shape of the considered domain is completely arbitrary. Furthermore, all quantities refer to an arbitrary coordinate system.

## 2.1 Warping function and stress function

A torque $M_x$ is subjected at the free end of the clamped rod. The torsion angle $\beta_x = \beta_x(x)$ is assumed to be small. As shown below only circular cross–sections are free of warping. In general the cross–sections do not remain plane under torsion, thus there are displacements $u_x$. The displacement field $\mathbf{u} = [u_x, u_y, u_z]^T$ is given by

$$u_x = \alpha\,\bar{\omega} \qquad u_y = -\beta_x\, z \qquad u_z = \beta_x\, y \tag{6}$$

where $\alpha = \beta_{x,x}$ and $\bar{\omega}(y,z)$ denotes the so–called warping function, respectively. Here, the constraint

$$\int_{(\Omega)} \bar{\omega}\,\mathrm{d}A = 0 \tag{7}$$

is required. The strains $\gamma_{xy}$ and $\gamma_{xz}$ are derived with (3). Hence, the shear stresses are given with material law $(4)_2$ and $(4)_3$

$$\tau_{xy} = G\alpha\,(\bar{\omega}_{,y} - z) \qquad\qquad \tau_{xz} = G\alpha\,(\bar{\omega}_{,z} + y)\,. \tag{8}$$

The other stresses are zero. Inserting (8) into the equation of equilibrium $(1)_1$ yields $G\alpha\,(\bar{\omega}_{,yy} + \bar{\omega}_{,zz}) = 0$. Furthermore, boundary conditions according to (2) have to be fulfilled.
Thus, the strong form of the boundary value problem is described by

$$\Delta\bar{\omega} = 0 \qquad \text{in } \Omega \qquad\qquad n_y\,\bar{\omega}_{,y} + n_z\,\bar{\omega}_{,z} = n_y z - n_z y \qquad \text{on } \partial\Omega \tag{9}$$

where $\Delta = (\cdot)_{,yy} + (\cdot)_{,zz}$ denotes the Laplace operator. This is the second boundary value problem of potential theory. The solution of the Neumann problem is unique up to an additive constant and represents a harmonic function which fulfills the boundary condition $(9)_2$. Closed form solutions are only available in some simple cases where the function of the boundary is given in the form $f(y,z) = 0$ with $\Delta f =$ constant. The normal vector of circular cross–sections at the boundary can be written as $\mathbf{n} = \mathbf{x}/|\mathbf{x}|$, where $\mathbf{x} = [y,\, z]^T$ denotes the position vector. In this case $n_y z - n_z y = 0$ holds. Hence, $\bar{\omega} = 0$ is exact solution of the differential equation and fulfills the boundary condition. This shows that circular cross–sections are free of warping.

Above boundary value problem in terms of $\bar{\omega}$ may be transformed introducing Prandtl's stress function $\Phi(y,z)$, see e.g. [9,10]. It is defined by

$$\Phi_{,z} = \bar{\omega}_{,y} - z \qquad\qquad -\Phi_{,y} = \bar{\omega}_{,z} + y\,. \tag{10}$$

Hence, the shear stresses are obtained by $\tau_{xy} = G\alpha\,\Phi_{,z}$ and $\tau_{xz} = -G\alpha\,\Phi_{,y}$. After some algebra one obtains

$$\Delta\Phi = -2 \qquad \text{in} \quad \Omega \qquad\qquad \Phi = \Phi_0 = \text{constant} \qquad \text{on} \quad \partial\Omega\,. \tag{11}$$

A constant does not influence the stresses; thus the boundary condition may be written as $\Phi_0 = 0$ on $\partial\Omega$. However for a multiple connected domain $\Phi$ may be set to zero along the outer boundary and $\Phi = \Phi_{0i} \neq 0$ along the inner boundaries, where $\Phi_{0i}$ takes different values at every inner boundary. For a hole $i$ the constant $\Phi_{0i}$ can not be chosen arbitrarily but is determined with the condition that the displacement field $u_x$ along the inner boundary must be continuous. This yields with (6) the following constraint

$$l(\Phi_{0i}) = \oint\limits_{(\partial\Omega_i)} u_{x,s}\,\mathrm{d}s \;=\; \alpha \oint\limits_{(\partial\Omega_i)} (-\bar{\omega}_{,y}\,n_z + \bar{\omega}_{,z}\,n_y)\,\mathrm{d}s \;=\; 0\,, \tag{12}$$

see also [9]. With (10) and integration by parts one obtains

$$l(\Phi_{0i}) = 2A_i + \oint\limits_{(\partial\Omega_i)} (\Phi_{,y}\,n_y + \Phi_{,z}\,n_z)\,\mathrm{d}s \;=\; 0\,, \tag{13}$$

where $A_i$ denotes the area of hole $i$. In general (13) cannot be solved explicitly for the unknown constants $\Phi_{0i}$ within a finite element analysis, but special techniques are necessary to fulfill constraints. Therefore, the use of the warping function is preferable, since (12) is automatically fulfilled if $\bar{\omega}$ is used as primary variable.

## 2.2 Torsion and warping constants

The warping function $\bar{\omega}$ is obtained as solution of the boundary value problem (9). The condition (7) is fulfilled by

$$\bar{\omega} = \omega - \frac{1}{A}\int\limits_{(\Omega)} \omega\,\mathrm{d}A\,. \tag{14}$$

The constant drops out when computing the derivatives of $\bar{\omega}$, therefore $\bar{\omega}$ can be replaced by $\omega$ in (9). Using $\bar{\omega}$ one can derive the coordinates $y_D$ and $z_D$ of the center of twist. This point is defined as point of rest in the pure torsion case. In this case the rod is free of normal forces and bending moments. For this purpose the transformation

$$\tilde{\omega} = \bar{\omega} + y_D\,\bar{z} - z_D\,\bar{y} \tag{15}$$

is introduced. From $u_x = \alpha\tilde{\omega}$ one computes the normal stress using $(3)_1$ and $(4)_1$ as $\sigma_x = E\alpha_{,x}\,\tilde{\omega}$. This is inserted into $N = M_z = M_y = 0$ with the definitions according to (5) which yields

$$\int\limits_{(\Omega)} \tilde{\omega}\,\mathrm{d}A = 0 \qquad \int\limits_{(\Omega)} \tilde{\omega} y\,\mathrm{d}A = 0 \qquad \int\limits_{(\Omega)} \tilde{\omega} z\,\mathrm{d}A = 0\,. \tag{16}$$

It is emphasized again that in general for the coupled bending torsion problem $\alpha_{,x} \neq 0$, whereas for the Saint–Venant torsion problem $\alpha_{,x} = 0$, thus $\sigma_x = 0$ holds. The coordinates $\bar{y}$ and $\bar{z}$ intersect at the centroid, thus considering (7) eq. $(16)_1$ is identically fulfilled. The unknown coordinates $y_D$ and $z_D$ follow from the conditions $(16)_2$ and $(16)_3$

$$\begin{aligned} \int\limits_{(\Omega)} \tilde{\omega} y \, \mathrm{d}A &= \int\limits_{(\Omega)} \tilde{\omega} \bar{y} \, \mathrm{d}A = \int\limits_{(\Omega)} (\bar{\omega}\bar{y} + y_D \bar{y}\bar{z} - z_D \bar{y}^2) \, \mathrm{d}A = 0 \\ \int\limits_{(\Omega)} \tilde{\omega} z \, \mathrm{d}A &= \int\limits_{(\Omega)} \tilde{\omega} \bar{z} \, \mathrm{d}A = \int\limits_{(\Omega)} (\bar{\omega}\bar{z} + z_D \bar{z}^2 - z_D \bar{y}\bar{z}) \, \mathrm{d}A = 0 \,. \end{aligned} \tag{17}$$

The solution of the linear system of equations yields

$$y_D = -\frac{A_{\bar{\omega}\bar{z}} \, A_{\bar{y}\bar{y}} - A_{\bar{\omega}\bar{y}} \, A_{\bar{y}\bar{z}}}{A_{\bar{y}\bar{y}} \, A_{\bar{z}\bar{z}} - A_{\bar{y}\bar{z}}^2} \qquad\qquad z_D = \frac{A_{\bar{\omega}\bar{y}} \, A_{\bar{z}\bar{z}} - A_{\bar{\omega}\bar{z}} \, A_{\bar{y}\bar{z}}}{A_{\bar{y}\bar{y}} \, A_{\bar{z}\bar{z}} - A_{\bar{y}\bar{z}}^2} \,. \tag{18}$$

It can be shown that the coordinates of the center of twist $\{y_D, z_D\}$ coincide with those of the center of shear $\{y_M, z_M\}$, see section 3.2. With (15) the warping constant $A_{\tilde{\omega}\tilde{\omega}}$ is defined

$$A_{\tilde{\omega}\tilde{\omega}} = \int\limits_{(\Omega)} \tilde{\omega}^2 \, \mathrm{d}A \,. \tag{19}$$

The torsion moment $M_x$ follows from integration of the shear stresses according to (5). Using the constitutive equation $M_x = G I_T \, \alpha$ yields the Saint–Venant torsion stiffness

$$\begin{aligned} I_T &= \int\limits_{(\Omega)} \left[ (\bar{\omega}_{,z} + y) y - (\bar{\omega}_{,y} - z) z \right] \mathrm{d}A \\ &= -\int\limits_{(\Omega)} (\Phi_{,y} \, y + \Phi_{,z} \, z) \, \mathrm{d}A \,. \end{aligned} \tag{20}$$

Alternative representations with $\omega$ or $\tilde{\omega}$ are possible. Integration by parts can be applied to $(20)_2$. For simply connected sections the boundary integral vanishes and one obtains $I_T = 2A_\Phi = 2 \int_{(\Omega)} \Phi \, \mathrm{d}A$.

# 3 Torsionless bending

In this section the rod is subjected to torsionless bending by moments $M_y$ and $M_z$. Different definitions on this term have been introduced in the literature, see Timoshenko and Goodier [9]. Here we apply the definition of Schwalbe [3] which yields the coordinates of the shear center. In this context Trefftz [4] introduced an energy criterion which leads essentially to the same results.

The problem of a cantilever with constant cross–section where a single load is applied at the end and parallel to one of the principal axes was solved by Saint–Venant, see [9]. Here, for numerical reasons the resulting boundary value problem is transformed which yields a Neumann problem. Furthermore, a split into two parts is presented. In this case the shear stresses are obtained by superposition.

## 3.1 Boundary value problem

The shape of the normal stresses $\sigma_x$ is assumed according to the elementary beam theory, thus linear with respect to $\bar{y}$ and $\bar{z}$. The other components of the stress tensor except the transverse shear stresses are neglected

$$\begin{aligned} \sigma_x &= \frac{M_y A_{\bar{y}\bar{y}} + M_z A_{\bar{y}\bar{z}}}{A_{\bar{y}\bar{y}} A_{\bar{z}\bar{z}} - A_{\bar{y}\bar{z}}^2}\,\bar{z} - \frac{M_z A_{\bar{z}\bar{z}} + M_y A_{\bar{y}\bar{z}}}{A_{\bar{y}\bar{y}} A_{\bar{z}\bar{z}} - A_{\bar{y}\bar{z}}^2}\,\bar{y} \\ \sigma_y &= \sigma_z = \tau_{yz} = 0\,. \end{aligned} \tag{21}$$

The derivative $\sigma_{x,x} = f_1(y,z)$ may be written as

$$f_1(y,z) = a_1\bar{y} + a_2\bar{z}\,, \tag{22}$$

where the constants are expressed with $M_{y,x} = Q_z$ and $M_{z,x} = -Q_y$ as

$$a_1 = \frac{Q_y A_{\bar{z}\bar{z}} - Q_z A_{\bar{y}\bar{z}}}{A_{\bar{y}\bar{y}} A_{\bar{z}\bar{z}} - A_{\bar{y}\bar{z}}^2} \qquad a_2 = \frac{Q_z A_{\bar{y}\bar{y}} - Q_y A_{\bar{y}\bar{z}}}{A_{\bar{y}\bar{y}} A_{\bar{z}\bar{z}} - A_{\bar{y}\bar{z}}^2}\,. \tag{23}$$

A stress function $\Psi$ is chosen

$$\tau_{xy} = \Psi_{,z} - \frac{1}{2}a_1\,\bar{y}^2 \qquad \tau_{xz} = -\Psi_{,y} - \frac{1}{2}a_2\,\bar{z}^2 \tag{24}$$

such that the equilibrium $(1)_1$ is identically fulfilled. Furthermore, the Beltrami compatibility conditions have to be satisfied

$$(1+\nu)\Delta\tau_{xy} + (\sigma_x + \sigma_y + \sigma_z)_{,xy} = 0 \qquad (1+\nu)\Delta\tau_{xz} + (\sigma_x + \sigma_y + \sigma_z)_{,xz} = 0\,, \tag{25}$$

where $\nu$ denotes Poisson's ratio. The other four compatibility equations of three–dimensional elasticity are identically fulfilled, see e.g Trefftz [4]. Substitution of (24) into (25) yields

$$\Delta\Psi_{,z} = \frac{\nu}{1+\nu}\,a_1 \qquad \Delta\Psi_{,y} = -\frac{\nu}{1+\nu}\,a_2\,. \tag{26}$$

Integration with respect to $y$ and $z$ defines the loading function

$$f_2(y,z) = \frac{\nu}{1+\nu}\left[a_2\,(y-y_0) - a_1(z-z_0)\right]. \tag{27}$$

The integration constants $y_0$ and $z_0$ are determined in section 3.3. Note, that $y - y_0 = \bar{y} - \bar{y}_0$ and the corresponding relation in $z$ hold.
The boundary conditions are described with (2) and (24)

$$(\Psi_{,z} - \frac{1}{2}a_1\bar{y}^2)\mathrm{d}z - (-\Psi_{,y} - \frac{1}{2}a_2\bar{z}^2)\mathrm{d}y = 0 \tag{28}$$

or

$$\mathrm{d}\Psi = \Psi_{,y}\,\mathrm{d}y + \Psi_{,z}\,\mathrm{d}z = \frac{1}{2}(a_1\bar{y}^2\mathrm{d}z - a_2\bar{z}^2\mathrm{d}y)\,. \tag{29}$$

Integration with respect to $y$ and $z$ yields along with (26) and (27) the Dirichlet problem

$$\Delta\Psi = -f_2(y,z) \quad \text{in} \quad \Omega \qquad\qquad \Psi(s) = h_1(s) \quad \text{on} \quad \partial\Omega \tag{30}$$

with $h_1(s) = \Psi_0 + \frac{1}{2}(a_1\bar{y}^2\bar{z} - a_2\bar{z}^2\bar{y})$ and $\Psi_0 =$ constant. We refer to the discussion on the boundary conditions for the stress function $\Phi$. Thus, for cross–sections with holes $\Psi_0$ may be set to zero along the outer boundary and $\Psi = \Psi_{0i} \neq 0$ along the inner boundaries, where $\Psi_{0i}$ takes different values at every inner boundary $i$. Eq. (29) can also be written as $\mathrm{d}\Psi = \frac{1}{2}(n_y a_1 \bar{y}^2 + n_z a_2 \bar{z}^2)\mathrm{d}s$ which shows that edges which are parallel to one of the coordinate axes have to be considered separately. In case, when $n_y$ or $n_z$ vanish the corresponding term cancels out and integration yields a constant. This makes clear, that above boundary condition is fairly difficult to implement in a finite element program, especially when automatic mesh generation is used.
Above Dirichlet problem can be transformed introducing the conjugate function $\bar{\Psi}$ by

$$\begin{aligned} \tau_{xy} &= \Psi_{,z} - \frac{1}{2}a_1\bar{y}^2 = \bar{\Psi}_{,y} - g_1(z) \\ \tau_{xz} &= -\Psi_{,y} - \frac{1}{2}a_2\bar{z}^2 = \bar{\Psi}_{,z} + g_2(y)\,, \end{aligned} \tag{31}$$

where

$$g_1(z) = -\frac{1}{2}\frac{\nu}{1+\nu}\,a_1\,(z - z_0)^2 \qquad\qquad g_2(y) = \frac{1}{2}\frac{\nu}{1+\nu}\,a_2\,(y - y_0)^2\,. \tag{32}$$

One can easily show that this substitution fulfills the Poisson equation $(30)_1$. The new differential equation in terms of $\bar{\Psi}$ follows from $\Psi_{,zy} - \Psi_{,yz} = 0$. Furthermore, the boundary conditions are derived from (2) and (31). One obtains the Neumann problem

$$\Delta\bar{\Psi} = -f_1(y,z) \quad \text{in} \quad \Omega \qquad\qquad n_y\bar{\Psi}_{,y} + n_z\bar{\Psi}_{,z} = n_y g_1(z) - n_z g_2(y) \quad \text{on} \quad \partial\Omega\,. \tag{33}$$

Furthermore, it can be shown that the integral of the shear stresses (31) yields the shear forces according to (5), see appendix A.1.

Finally, the decomposition

$$\Psi = \Psi_1 + \Psi_2 \qquad\qquad \bar{\Psi} = \bar{\Psi}_1 + \bar{\Psi}_2 \tag{34}$$

is useful for further considerations where the functions $\Psi_1, \Psi_2$ and $\bar{\Psi}_1, \bar{\Psi}_2$ fulfill

**Problem A:**

$$\begin{aligned} &\Delta\Psi_1 = 0 \quad \text{in} \quad \Omega \qquad \Psi_1(s) = h_1(s) \quad \text{on} \quad \partial\Omega \\ &\Delta\bar{\Psi}_1 = -f_1(y,z) \qquad\quad\; n_y\bar{\Psi}_{1,y} + n_z\bar{\Psi}_{1,z} = 0 \end{aligned}$$

**Problem B:**

$$\begin{aligned} &\Delta\Psi_2 = -f_2(y,z) \quad \text{in} \quad \Omega \qquad \Psi_2 = \Psi_0 \quad \text{on} \quad \partial\Omega \\ &\Delta\bar{\Psi}_2 = 0 \qquad\qquad\quad\; n_y\bar{\Psi}_{2,y} + n_z\bar{\Psi}_{2,z} = n_y g_1(z) - n_z g_2(y) \end{aligned} \tag{35}$$

It can be seen that the decomposition satisfies the original equations (30) and (33). In the following the indices 1 and 2 refer to problem $A$ and $B$, respectively.

## 3.2 Problem A: Shear stresses

The shear stresses $\tau_{1xy}$ and $\tau_{1xz}$ are obtained from the stress functions of the boundary value problem $A$ by partial derivatives

$$\tau_{1xy} = \Psi_{1,z} - \frac{1}{2} a_1 \bar{y}^2 = \bar{\Psi}_{1,y} \qquad \tau_{1xz} = -\Psi_{1,y} - \frac{1}{2} a_2 \bar{z}^2 = \bar{\Psi}_{1,z} \; . \tag{36}$$

It can be shown according to appendix A.1 setting $g_1(z) = g_2(y) = 0$ that

$$\int\limits_{(\Omega)} \tau_{1xy} \, \mathrm{d}A = Q_y \qquad \int\limits_{(\Omega)} \tau_{1xz} \, \mathrm{d}A = Q_z \tag{37}$$

holds. This makes clear that the shear stresses $\tau_{1xy}$ and $\tau_{1xz}$ are necessary to fulfill the equilibrium equations and to set up the shear forces.
The center of shear $M$ is defined as place where the torsion moment in terms of above derived shear stresses vanishes. Hence, the coordinates $\{y_M, z_M\}$ follow from the condition

$$Q_z \, y_M - Q_y \, z_M = \int\limits_{(\Omega)} (\tau_{xz} y - \tau_{xy} z) \, \mathrm{d}A \, . \tag{38}$$

Here, only the shear stresses $\tau_{1xy}$ and $\tau_{1xz}$ contribute to this equation. The torsion moment of the additional shear stresses following from problem B is zero. It can be shown that the coordinates of the center of twist and of shear coincide, thus

$$y_M = y_D \qquad z_M = z_D \, , \tag{39}$$

where $\{y_D, z_D\}$ are given in (18). For a proof we refer to appendix A.2. The fact that both centers coincide was first recognized by Weber [2] applying the Betty–Maxwell reciprocal relations.

**Remark:**
The associated displacement field reads

$$\begin{aligned} u_x &= \beta_y(x) \, \bar{z} - \beta_z(x) \, \bar{y} + \psi(y,z) \\ u_y &= v(x) \\ u_z &= w(x) \, , \end{aligned} \tag{40}$$

where $\beta_y(x)$ and $\beta_z(x)$ denote the rotations about $y$ and $z$. Furthermore, $v(x)$ and $w(x)$ describe the deflections of the reference point in $y$ and $z$–direction, respectively. The customary beam kinematic with inextensibility in transverse directions and plane cross–sections is extended using the warping function $\psi(y,z)$. The strains are obtained with (3) by partial derivatives of the displacement field

$$\begin{aligned} \varepsilon_x &= \beta_{y,x} \, \bar{z} - \beta_{z,x} \, \bar{y} \\ \gamma_{xy} &= (\beta_z + v_{,x}) + \psi_{,y} \\ \gamma_{xz} &= (\beta_y + w_{,x}) + \psi_{,z} \; . \end{aligned} \tag{41}$$

Inserting the equations of elasticity (4) considering (41) into the equilibrium $(1)_1$ yields $\sigma_{x,x} = -G\,(\psi_{,yy} + \psi_{,zz})$. The expression $\sigma_{x,x} = E\,(\beta_{y,xx}\,\bar{z} - \beta_{z,xx}\,\bar{y})$ is reformulated with

the bending moments according to (5) and $M_{y,x} = Q_z$, $M_{z,x} = -Q_y$. After some algebra one obtains $\sigma_{x,x} = f_1(y,x)$ where $f_1(y,z)$ is given with eq. (22).
Introducing $\bar{\psi}$ by

$$\bar{\psi} = \psi + c_1\,\bar{y} + c_2\,\bar{z}\,, \tag{42}$$

where the constants $c_1$ und $c_2$ follow from conditions (37) with $\bar{\Psi}_1 = G\bar{\psi}$

$$c_1 = \frac{Q_y}{GA} - \frac{1}{A}\int\limits_{(\Omega)} \psi_{,y}\,\mathrm{d}A \qquad\qquad c_2 = \frac{Q_z}{GA} - \frac{1}{A}\int\limits_{(\Omega)} \psi_{,z}\,\mathrm{d}A\,. \tag{43}$$

Thus, the underlying boundary value problem in terms of $\bar{\Psi}_1$ is given in (35). Since inextensibility is assumed with the kinematic assumption (40) the ratio $E/G = 2(1+\nu)$ is not contained in above equations.

### 3.3 Problem B: Additional shear stresses

The additional shear stresses are necessary to satisfy the compatibility equations and follow from the solution of problem $B$

$$\tau_{2xy} = \Psi_{2,z} = \bar{\Psi}_{2,y} - g_1(z) \qquad\qquad \tau_{2xz} = -\Psi_{2,y} = \bar{\Psi}_{2,z} + g_2(y)\,. \tag{44}$$

Furthermore, the constraints

$$\int\limits_{(\Omega)} \tau_{2xy}\,\mathrm{d}A = 0 \qquad \int\limits_{(\Omega)} \tau_{2xz}\,\mathrm{d}A = 0 \qquad \int\limits_{(\Omega)} (\tau_{2xz}y - \tau_{2xy}z)\mathrm{d}A = 0 \tag{45}$$

must hold. It can be shown that the first two equations are fulfilled. The proof can be carried out according to appendix A.1 with $f_1(y,z) = 0$. The third condition demands that for torsionless bending the torsion moment of the additional shear stresses vanishes. From this condition the integration constants $y_0$ and $z_0$ are derived inserting the shear stresses (44) and $y = -(\Phi_{,y} + \bar{\omega}_{,z})$, $z = -(\Phi_{,z} - \bar{\omega}_{,y})$ using (10)

$$\int\limits_{(\Omega)} (\tau_{2xz}y - \tau_{2xy}z)\mathrm{d}A = \int\limits_{(\Omega)} [(\bar{\Psi}_{2,y} - g_1)(\Phi_{,z} - \bar{\omega}_{,y}) - (\bar{\Psi}_{2,z} + g_2)(\Phi_{,y} + \bar{\omega}_{,z})]\mathrm{d}A\,. \tag{46}$$

This is rewritten as follows

$$\begin{aligned}
&\int\limits_{(\Omega)} (\tau_{2xz}y - \tau_{2xy}z)\mathrm{d}A \\
= &\int\limits_{(\Omega)} (\bar{\Psi}_{2,y}\,\Phi_{,z} - \bar{\Psi}_{2,z}\,\Phi_{,y})\mathrm{d}A - \oint\limits_{(\partial\Omega)} (n_y\Phi_{,z} - n_z\Phi_{,y})\,\bar{\Psi}_2\,\mathrm{d}s \\
&- \int\limits_{(\Omega)} [(\bar{\Psi}_{2,y} - g_1)\bar{\omega}_{,y} + (\bar{\Psi}_{2,y} + g_2)\bar{\omega}_{,z}]\,\mathrm{d}A + \oint\limits_{(\partial\Omega)} [n_y(\bar{\Psi}_{2,y} - g_1) + n_z(\bar{\Psi}_{2,y} + g_2))]\,\bar{\omega}\mathrm{d}s \\
&- \int\limits_{(\Omega)} (g_1\Phi_{,z} + g_2\Phi_{,y})\,\mathrm{d}A\,.
\end{aligned} \tag{47}$$

The boundary integrals vanish considering (35), $(9)_2$ and (10). Next, Green's formula is applied

$$\begin{aligned}&\int\limits_{(\Omega)} (\tau_{2xz} y - \tau_{2xy} z)\mathrm{d}A \\ &= \int\limits_{(\Omega)} (\Phi_{,yz} - \Phi_{,zy})\,\bar{\Psi}_2\,\mathrm{d}A + \int\limits_{(\Omega)} \Delta\bar{\Psi}_2\,\bar{\omega}\,\mathrm{d}A - \int\limits_{(\Omega)} (g_1\Phi_{,z} + g_2\Phi_{,y})\,\mathrm{d}A\,.\end{aligned} \tag{48}$$

The first integral is obviously zero. The same holds for the second integral when taking (35) into account. Thus, inserting the functions $g_1(z)$ and $g_2(y)$ from (32) into the third integral we obtain

$$\int\limits_{(\Omega)} (\tau_{2xz} y - \tau_{2xy} z)\mathrm{d}A = \frac{1}{2}\frac{\nu}{1+\nu} \int\limits_{(\Omega)} [\Phi_{,z}\, a_1 (z - z_0)^2 - \Phi_{,y}\, a_2 (y - y_0)^2]\,\mathrm{d}A = 0\,. \tag{49}$$

Next, the following definitions are introduced

$$\begin{aligned} B_y &:= \int\limits_{(\Omega)} (-\Phi_{,y})\, y\,\mathrm{d}A &&= \int\limits_{(\Omega)} (\bar{\omega}_{,z} + y)\, y\,\mathrm{d}A \\ B_{yy} &:= \int\limits_{(\Omega)} (-\Phi_{,y})\, y^2\,\mathrm{d}A &&= \int\limits_{(\Omega)} (\bar{\omega}_{,z} + y)\, y^2\,\mathrm{d}A \\ B_z &:= \int\limits_{(\Omega)} \Phi_{,z}\, z\,\mathrm{d}A &&= \int\limits_{(\Omega)} (\bar{\omega}_{,y} - z)\, z\,\mathrm{d}A \\ B_{zz} &:= \int\limits_{(\Omega)} \Phi_{,z}\, z^2\,\mathrm{d}A &&= \int\limits_{(\Omega)} (\bar{\omega}_{,y} - z)\, z^2\,\mathrm{d}A\,. \end{aligned} \tag{50}$$

The resultants of the torsion shear stresses vanish

$$\int\limits_{(\Omega)} \Phi_{,z}\ \mathrm{d}A = 0 \qquad\qquad \int\limits_{(\Omega)} \Phi_{,y}\ \mathrm{d}A = 0\,. \tag{51}$$

The proof can be carried out in an analogous way to appendix A.1 considering eq. (9) and (10), see also Sokolnikoff [10].
Inserting (50) and (51) into eq. (49) yields

$$\frac{1}{2}\frac{\nu}{1+\nu}\left[a_1\left(B_{zz} - 2z_0 B_z\right) + a_2\left(B_{yy} - 2y_0 B_y\right)\right] = 0\,. \tag{52}$$

The constants $a_1$ and $a_2$ according to (23) are not zero. Therefore, eq. (52) can only be fulfilled if the terms in both brackets vanish which yields

$$y_0 = \frac{B_{yy}}{2B_y} \qquad\qquad z_0 = \frac{B_{zz}}{2B_z}\,. \tag{53}$$

In case of simply connected sections with $\Phi_0 = 0$ along the boundary integration by parts yields

$$y_0 = \frac{A_{\Phi y}}{A_\Phi} \qquad\qquad z_0 = \frac{A_{\Phi z}}{A_\Phi}\,. \tag{54}$$

This gives the centroid of a body which is described by the stress function $\Phi$. Another representation with $\bar{y}_0 = A_{\Phi\bar{y}}/A_\Phi$ and $\bar{z}_0 = A_{\Phi\bar{z}}/A_\Phi$ is possible. If $z$ is symmetry axis $y_0 = 0$ holds and vice versa. Assuming principal axes the constants have been derived by Trefftz [4] in terms of (54) using an energy criterion.
Eq. (53) also holds for multiple connected sections. Furthermore, we can use the warping function $\bar{\omega}$ to evaluate the integrals (50). Thus, the difficulties which occur with the stress function $\Phi$ discussed in section 2 can be avoided.

# 4 Finite element formulation

## 4.1 Weak form of the boundary value problem

We consider the differential equation with Dirichlet or Neumann boundary conditions

$$\begin{aligned} \Delta\varphi = -f(y,z) \quad \text{in} \quad \Omega \qquad & n_y\varphi_{,y} + n_z\varphi_{,z} = g(y,z) \qquad \text{on} \quad \partial\Omega \\ \text{or} \quad & \varphi(s) = h(s)\,, \end{aligned} \tag{55}$$

where $\varphi(y,z)$ represents the warping functions and stress functions of the previous sections. The functions $f(y,z)$, $g(y,z)$ and $h(s)$ are given for the cases torsion and bending in table 1. The weak form of the boundary value problem (55) is obtained weighting the differential equation with test functions $\eta \in \mathcal{V}$ with

$$\mathcal{V} = \{\eta \in H^1(\Omega), \eta = 0 \text{ on } \partial\Omega_\varphi\}\,, \tag{56}$$

where $\partial\Omega_\varphi$ denotes the part of the boundary with prescribed values of $\varphi$. Integration over the domain $\Omega$ yields

$$G(\varphi,\eta) = -\int\limits_{(\Omega)} \left[\varphi_{,yy} + \varphi_{,zz} + f(y,z)\right]\,\eta\,\mathrm{d}A = 0\,. \tag{57}$$

Integration by parts and inserting the Neumann boundary condition $(55)_2$ leads to

$$G(\varphi,\eta) = \int\limits_{(\Omega)} \left[\varphi_{,y}\,\eta_{,y} + \varphi_{,z}\,\eta_{,z}\right]\,\mathrm{d}A - \int\limits_{(\Omega)} f(y,z)\,\eta\,\mathrm{d}A - \oint\limits_{(\partial\Omega)} g(y,z)\eta\,\mathrm{d}s = 0\,. \tag{58}$$

In case of Dirichlet boundary conditions the boundary integral vanishes since the test functions are zero along the boundary, see eq. (56). The weak form must be fulfilled for *all* admissible functions $\eta \in \mathcal{V}$, thus it is equally good to (55).
The shear stresses due to torsion are given here for $G\alpha = 1$. For the bending case the boundary value problem can be separated into two parts. If e.g. the split into $\bar{\Psi}_1$ and $\Psi_2$ is chosen one obtains the total shear stresses

$$\tau_{xy} = \bar{\Psi}_{1,y} + \Psi_{2,z} \qquad\qquad \tau_{xz} = \bar{\Psi}_{1,z} - \Psi_{2,y} \tag{59}$$

by superposition.

**Remark:**
A split of the boundary value problem into a part which fulfills the equlibrium and a

**Table** 1: Summary of the warping functions and stress functions

| problem | $\varphi(y,z)$ | $\tau_{xy}$ | $\tau_{xz}$ | $f(y,z)$ | $g(y,z)$ | $h(s)$ |
|---|---|---|---|---|---|---|
| torsion | $\bar{\omega}$ | $\bar{\omega}_{,y} - z$ | $\bar{\omega}_{,z} + y$ | 0 | $n_y z - n_z y$ | – |
| | $\Phi$ | $\Phi_{,z}$ | $-\Phi_{,y}$ | 2 | – | $\Phi_0$ |
| bending | $\Psi$ | $\Psi_{,z} - \frac{1}{2}a_1\bar{y}^2$ | $-\Psi_{,y} - \frac{1}{2}a_2\bar{z}^2$ | $f_2(y,z)$ | – | $h_1(s)$ |
| | $\bar{\Psi}$ | $\bar{\Psi}_{,y} - g_1(z)$ | $\bar{\Psi}_{,z} + g_2(y)$ | $f_1(y,z)$ | $n_y g_1(z) - n_z g_2(y)$ | – |
| | $\Psi_1$ | $\Psi_{1,z} - \frac{1}{2}a_1\bar{y}^2$ | $-\Psi_{1,y} - \frac{1}{2}a_2\bar{z}^2$ | 0 | – | $h_1(s)$ |
| | $\bar{\Psi}_1$ | $\bar{\Psi}_{1,y}$ | $\bar{\Psi}_{1,z}$ | $f_1(y,z)$ | 0 | – |
| | $\Psi_2$ | $\Psi_{2,z}$ | $-\Psi_{2,y}$ | $f_2(y,z)$ | – | $\Psi_0$ |
| | $\bar{\Psi}_2$ | $\bar{\Psi}_{2,y} - g_1(z)$ | $\bar{\Psi}_{2,z} + g_2(y)$ | 0 | $n_y g_1(z) - n_z g_2(y)$ | – |

part which describes the effect of Poisson's ratio has been proposed by Weber [1]. The stress functions introduced in [1] correspond with $\bar{\Psi}_1$ and $\Psi_2$. Schwalbe introduced stress functions which can be compared with $\Psi_1$ and $\Psi_2$ whereas the stress function of Trefftz corresponds with $\Psi$. The authors of [1], [3] and [4] restrict themselves to coordinates which describe principal axes of the cross–section.
In this paper we introduce the conjugate function $\bar{\Psi}$ which leads to a Neumann problem. Furthermore, the coordinates are not restricted to principal axes. It is emphasized again that the Neumann boundary conditions described by $g(y,z)$ are easier to implement in a finite element program. As is shown in section 3.2 $\bar{\Psi}_1$ describes warping of the cross–section due to bending. Thus, $\bar{\Psi}_2$ and $\bar{\Psi}$ are also warping functions. Therefore, continuity conditions around holes as are discussed in section 2.1 are automatically fulfilled. This is not the case when using the stress functions $\Psi, \Psi_1$ and $\Psi_2$. The bending shear stresses of the examples in section 5 are obtained by differentiation of the warping function $\bar{\Psi}$.

## 4.2 Stiffness matrix and load vector

The weak form of the boundary value problem (58) can be solved approximately using the finite element method. Since only derivatives of first order occur, $C^0$–continuous elements can be used for the finite element discretization. For this purpose the coordinates $\mathbf{x} = [y,z]^T$, the unknown function $\varphi$ and the test function $\eta$ are interpolated within a typical element using the same shape functions

$$\mathbf{x}^h = \sum_{I=1}^{nel} N_I(\xi,\eta)\,\mathbf{x}_I \qquad \varphi^h = \sum_{I=1}^{nel} N_I(\xi,\eta)\,\varphi_I \qquad \eta^h = \sum_{I=1}^{nel} N_I(\xi,\eta)\,\eta_I\,, \tag{60}$$

where *nel* denotes the number of nodes per element. The index $h$ is used to denote the approximate solution of the finite element method. The derivatives of the shape functions $N_I(\xi,\eta)$ with respect to $y$ and $z$ are obtained in a standard way using the chain rule. Inserting the derivatives of $\varphi^h$ and $\eta^h$ into the weak form (58) yields the finite element equation

$$G(\varphi^h,\eta^h) = \mathop{\mathsf{A}}_{e=1}^{numel} \sum_{I=1}^{nel}\sum_{K=1}^{nel} \eta_I\,(K^e_{IK}\,\varphi_K - P^e_I) = 0\,. \tag{61}$$

Here, $\mathop{\mathbf{A}}$ denotes the assembly operator with *numel* the total number of elements to discretize the problem. The contribution of nodes $I$ and $K$ to the stiffness matrix and of node $I$ to the load vector reads

$$K^e_{IK} = \int\limits_{(\Omega_e)} (N_{I,y}\, N_{K,y} + N_{I,z}\, N_{K,z}\,)\,\mathrm{d}A_e \qquad P^e_I = \int\limits_{(\Omega_e)} f(y,z)\, N_I\,\mathrm{d}A_e + \int\limits_{(\partial\Omega)} g(y,z)\, N_I\,\mathrm{d}s\,, \tag{62}$$

where the functions $f(y,z)$ and $g(y,z)$ are given in table 1. The section quantities $A, A_{\bar{y}\bar{y}}, A_{\bar{z}\bar{z}}, A_{\bar{y}\bar{z}}$ and the coordinates $y_S, z_S$ must be known for the computation of the flexural shear stresses. This can be achieved using a finite element solution, see [18]. The constants $y_0$ and $z_0$ are obtained from (53).
Since the tangent vector $\mathbf{t}$ and the outward normal vector $\mathbf{n}$ form a right–handed system the direction of the coordinate $s$ at inner and outer boundaries is uniquely defined. The chain rule yields the differential arc length $\mathrm{d}s = |\mathbf{x}|\mathrm{d}\xi$ with the normalized coordinate $-1 \le \xi \le +1$. The derivative of $N_I$ with respect to $s$ reads $N_{I,s} = N_{I,\xi}\,/|\mathbf{x}|$. Now the unit tangent vector $\mathbf{t}$ and the normal vector $\mathbf{n}$ using the condition $\mathbf{n}^T\mathbf{t} = 0$ are expressed

$$\mathbf{t} = \begin{bmatrix} t_y \\ t_z \end{bmatrix} = \sum_{I=1}^{nel} N_{I,s}\ \mathbf{x}_I \qquad\qquad \mathbf{n} = \begin{bmatrix} -t_z \\ t_y \end{bmatrix}. \tag{63}$$

Eq. (61) leads to a linear system of equation. Furthermore, boundary conditions $\varphi(s) = h(s)$ according to table 1 have to be considered. In case of Neumann boundary conditions the value $\varphi_I$ of one arbitrary nodal point $I$ has to be suppressed.

## 4.3 Adaptive mesh refinement

In the following we briefly comment on the adaptive mesh refinement within the h–method for isoparametric 4–node elements. At first a starting mesh considering a–priori–criteria is generated. These criteria are deviations of the element geometry from a square and deviations of the approximated geometry from the exact geometry of the boundary. The Zienkiewicz–Zhu indicator [19] is applied for further mesh refinement. Although this indicator is not an error estimator with bounds numerical tests show that it can be effectively used to steer the adaptive mesh refinement. It is assumed, that the error of the shear stresses $\mathbf{e}_\tau = \boldsymbol{\tau} - \boldsymbol{\tau}^h$ with respect to the exact solution $\boldsymbol{\tau}$ can be described approximately by $\tilde{\mathbf{e}}_\tau = \tilde{\boldsymbol{\tau}} - \boldsymbol{\tau}^h$. Here, $\boldsymbol{\tau}^h$ denotes the vector of shear stresses computed from the warping functions or stress functions, see table 1. Furthermore, the shear stresses $\tilde{\boldsymbol{\tau}}$ are obtained with bi–linear shape functions $\mathbf{N}_e$ from the nodal values $\hat{\boldsymbol{\tau}}$ by $\tilde{\boldsymbol{\tau}} = \mathbf{N}_e\hat{\boldsymbol{\tau}}$ in $\Omega_e$, thus are continuous across the element boundaries. The nodal stresses are computed using the minimum condition

$$\mathop{\mathbf{A}}_{e=1}^{numel} \int\limits_{(\Omega_e)} (\tilde{\boldsymbol{\tau}} - \boldsymbol{\tau}^h)^T(\tilde{\boldsymbol{\tau}} - \boldsymbol{\tau}^h)\,\mathrm{d}A_e \longrightarrow \min\,. \tag{64}$$

The procedure can be seen as a $L_2$–smoothing process within the domain $\Omega$. The associated minimum condition

$$\mathop{\mathbf{A}}_{e=1}^{numel} \left[ \int\limits_{(\Omega_e)} \mathbf{N}_e^T\mathbf{N}_e\,\mathrm{d}A_e\ \hat{\boldsymbol{\tau}} - \int\limits_{(\Omega_e)} \mathbf{N}_e^T\boldsymbol{\tau}^h\,\mathrm{d}A_e \right] = 0 \tag{65}$$

represents a linear system of equation for the unknown nodal stresses $\hat{\boldsymbol{\tau}}$.
The local error of an element $\eta_e = e_{\Omega_e}/e_\Omega$ with the error of the considered element $e^2_{\Omega_e} = \int_{(\Omega_e)} (\tilde{\boldsymbol{\tau}} - \boldsymbol{\tau}^h)^T (\tilde{\boldsymbol{\tau}} - \boldsymbol{\tau}^h)\, \mathrm{d}A_e$ and the averaged error of the total domain $e_\Omega$ serves as density function to steer the refinement of the finite element mesh. Within the chosen hierarchical refinement each element which has to be refined is subdivided into four subelements. So–called hanging nodes at the boundaries of the refined subdomains are avoided using special refinement strategies. If the solution is sufficient smooth the refinement process is repeated for $\eta_e > 0.03 - 0.05$.

# 5 Examples

The presented finite element formulation has been implemented into an enhanced version of the program FEAP. A documentation of the basis version may be found in the book of Zienkiewicz und Taylor [20]. The Saint–Venant torsion modulus computed from $(20)_1$ is denoted by $I_{T1}$ whereas the value obtained from $(20)_2$ is denoted by $I_{T2}$. Due to the different boundary conditions the number of unknowns $N$ to compute $I_{T1}$ is only approximately equal the number for $I_{T2}$. At inner corners without rounding the shear stresses are unbounded. The below presented plots show the distribution for a chosen mesh density. Further mesh refinement influences the results only in the direct vicinity of the singularity.

## 5.1 Rectangular cross–section

The first example is concerned with a rectangular cross–section, see Fig. 2. In the following the distribution of the shear stresses due to a shear force $Q_z$ is investigated. Within the elementary beam theory the shear stresses $\tau_{xz}$ are given according to the quadratic parabola $\tau_{xz} = \tau^*[1 - (2\,z/h)^2]$ with $\tau^* = 3Q_z/(2A)$.

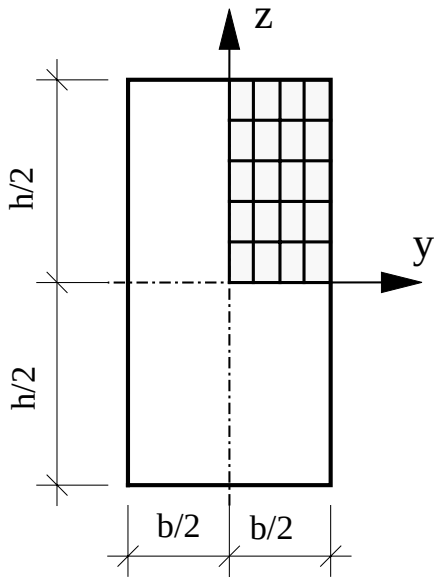


**Figure** 2: Rectangular cross–section

**Table** 2: Correction factors for the shear stresses of a rectangular cross–section ($\nu = 0.25$)

| h/b | 2 | 1 | 0.5 | 0.25 |
|---|---|---|---|---|
| z=0, y=0 | 0.983 | 0.940 | 0.856 | 0.805 |
| z=0, y =b/2 | 1.033 | 1.126 | 1.396 | 1.988 |

Considering symmetry one quarter is discretized by $n \times n$ 4–noded elements. With Poisson's ratio $\nu = 0$ one obtains the finite element solution $\tau_{xy} = 0$ and shear stresses $\tau_{xz}$ which are constant in y–direction. For $n = 5$ there is practically agreement with the beam solution. For the additional shear stresses a solution has been evaluated by Timoshenko and Goodier [9] using Fourier series. The finite element solution of two points for $\nu = 0.25$ and different ratios of $h/b$ is given in table 2. It corresponds with the series

solution published in [9]. The above defined maximum shear stress $\tau^*$ of the elementary beam theory has to be multiplied with the factors of the table to get the correct stresses at the specified points. For a square cross–section the error in the maximum stress of the elementary beam theory is about 13 %. Plots of the normalized shear stresses $\tau_{xz}/\tau^*$ for a square are given in Fig. 3 and the distribution along $z = 0$ in Fig. 4. For $\nu = 0$ one obtains the elementary beam solution with the parabolic shape in z–direction. The stress concentration at $z = 0, y = \pm b/2$ for $\nu = 0.25$ can be seen clearly.

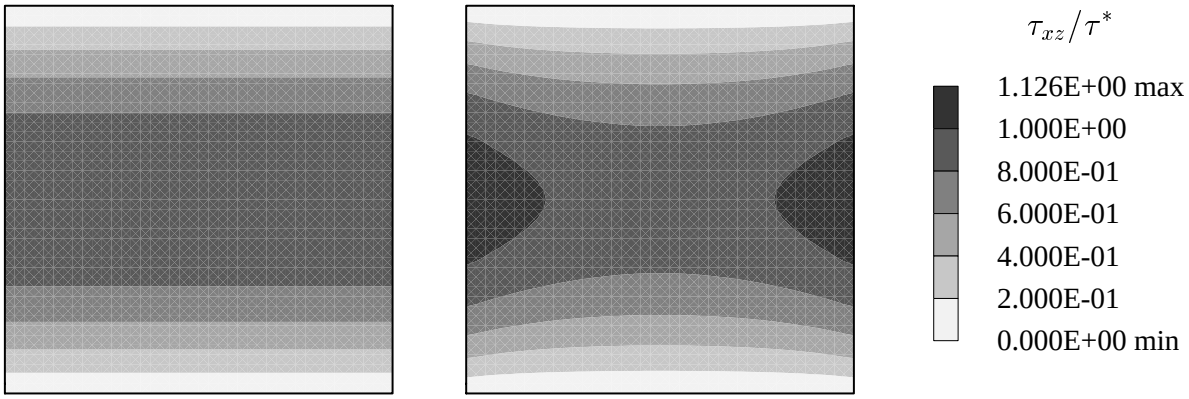


**Figure** 3: Normalized shear stresses for a square cross–section

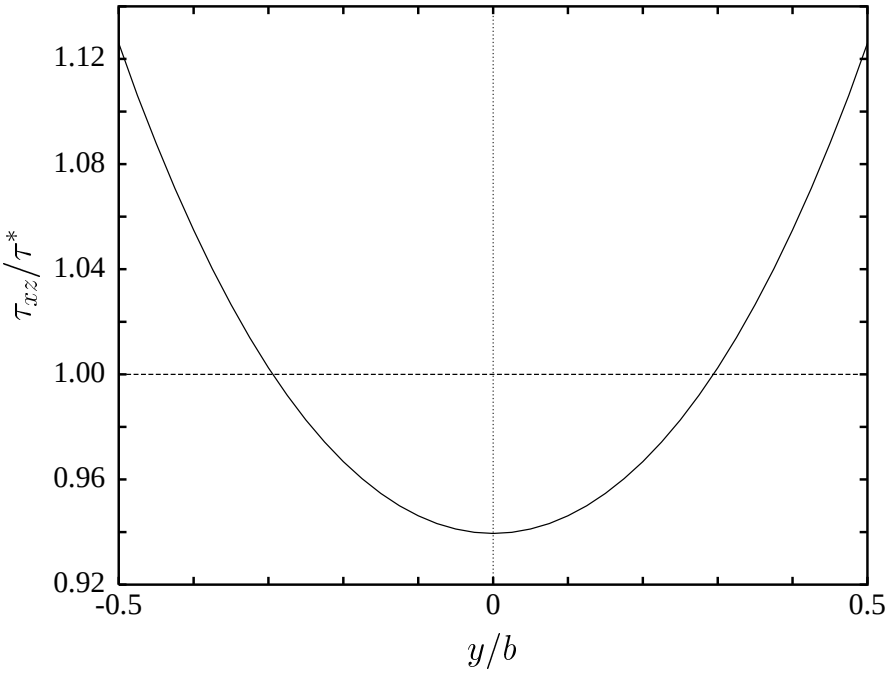


**Figure** 4: Normalized shear stresses at $z = 0$ for a square cross–section with $\nu = 0.25$

## 5.2 Cross–section with varying width

The next example is concerned with a cross–section with varying width, see Fig. 5. Again the shear stresses due to a shear force $Q_z = -1\,kN$ are computed. The geometrical data are $a = 10\,cm$ and $e = 5/3\,a$. From the elementary beam theory the stress flux

$$t_z(z = e) = \int_{-2a}^{2a} \tau_{xz} \mathrm{d}y = \frac{Q_z A_z(z)}{A_{\bar{z}\bar{z}}} = -37.9 \cdot 10^{-3}\,kN/cm$$

can be evaluated. Considering symmetry half of the cross–section is discretized with 240 elements. Using trapezoidal rule we obtain the resultant $t_z(z = z_s) = -37.8 \cdot 10^{-3}\,kN/cm$ for $\nu = 0$ which is approximately the beam solution. Fig. 6 shows a plot of the shear stresses $\tau_{xz}$ for $\nu = 0$ and $\nu = 0.2$. The distribution in y–direction deviates considerably from a constant shape. With further mesh refinement one recognizes a singularity at the inner corner. Finally, a plot of the resulting shear stresses is depicted in Fig. 7.

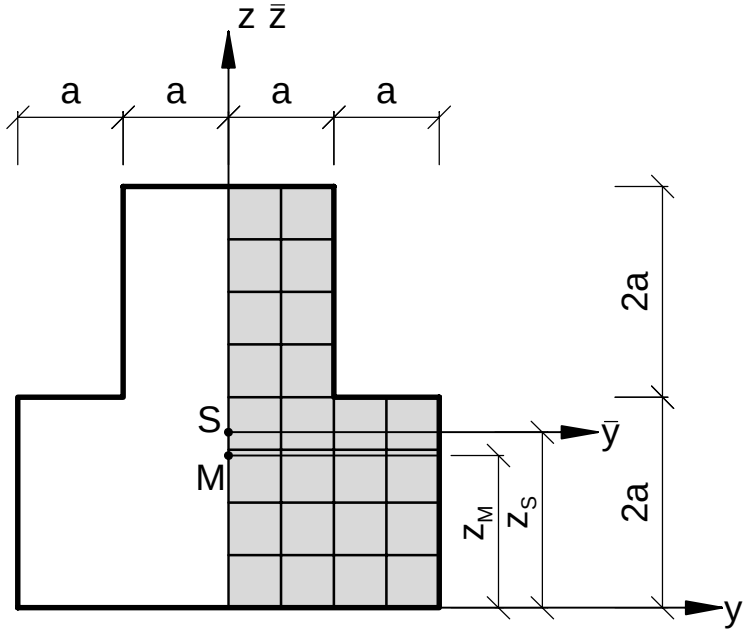


**Figure** 5: Cross–section with varying width

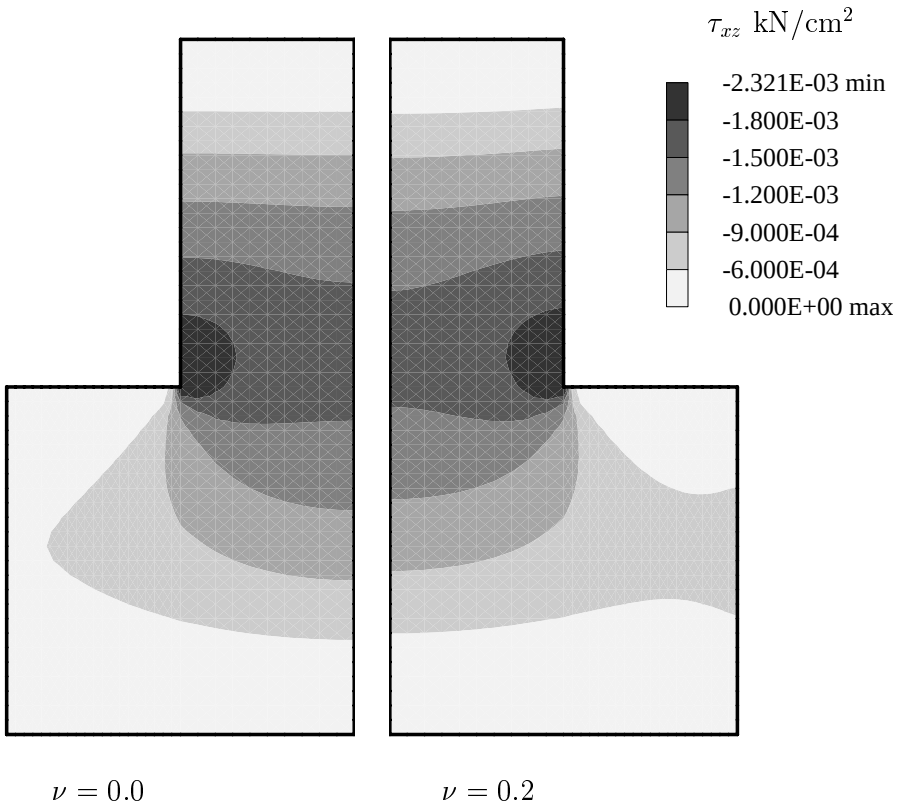


**Figure** 6: Plot of shear stresses $\tau_{xz}$

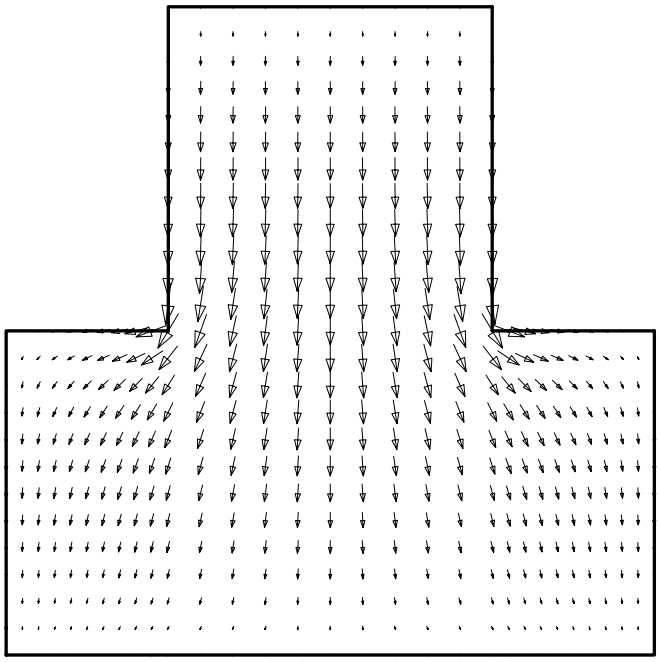

**Figure** 7: Resulting shear stresses for $\nu = 0.2$

## 5.3 Crane rail A 100

The cross–section of a crane rail A100 according to the German code DIN 536 is investigated. The geometrical data are given in DIN 536 (9.91). Considering symmetry one half of the cross–section with an adaptive refined mesh for a shear force $Q_z$ is depicted in Fig. 8. The torsion and warping constants which have been defined in section 2 are given in table 3 for adaptive mesh refinement and for uniform refinement. The warping function $\tilde{w}$ is plotted in Fig. 9 and the resulting torsion shear stresses in Fig. 10, respectively.
Next, shear stresses due to $Q_y = 1\,kN$ and $Q_z = -1\,kN$ are evaluated. From eq. $(53)_2$ we evaluate the constant $z_0 = 5.078\,cm$. With $Q_z = 0$ the coordinate $z_M = 3.252\,cm$ is computed from eq. (38), thus $z_M = z_D$ is verified numerically. As Fig. 11 shows there is a considerable stress concentration in the cross–section. There are only minor differences for the two ratios $\nu = 0$ and $\nu = 0.3$. The resulting shear stresses are plotted for $\nu = 0.3$ in Fig. 12 and Fig. 13 for the respective shear force.

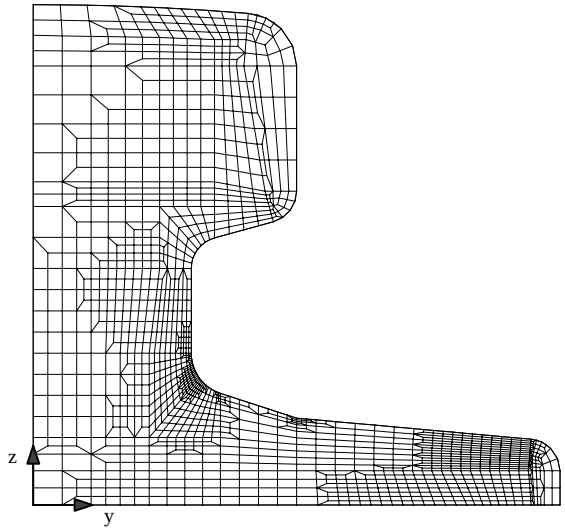


**Figure** 8: Discretization of a crane rail, adaptive refined mesh for $Q_z$

**Table** 3: Torsion and warping properties of a crane rail A100

| adaptive mesh refinement | | | | |
|---|---|---|---|---|
| $N$ | $I_{T1}$ $cm^4$ | $I_{T2}$ $cm^4$ | $A_{\tilde{w}\tilde{w}}$ $cm^6$ | $z_D$ $cm$ |
| 90 | 683.3 | 638.4 | 3838 | 3.262 |
| 304 | 674.0 | 662.4 | 3954 | 3.254 |
| 1035 | 671.5 | 668.6 | 3981 | 3.254 |
| 3056 | 670.9 | 670.0 | 3989 | 3.253 |
| 5550 | 670.7 | 670.4 | 3990 | 3.252 |
| 7635 | 670.7 | 670.4 | 3992 | 3.252 |
| 8998 | 670.7 | 670.5 | 3993 | 3.252 |

| uniform mesh refinement | | | | |
|---|---|---|---|---|
| $N$ | $I_{T1}$ $cm^4$ | $I_{T2}$ $cm^4$ | $A_{\tilde{w}\tilde{w}}$ $cm^6$ | $z_D$ $cm$ |
| 90 | 683.3 | 638.4 | 3838 | 3.262 |
| 304 | 674.0 | 662.4 | 3954 | 3.254 |
| 1106 | 671.5 | 668.6 | 3984 | 3.252 |
| 4270 | 670.9 | 670.1 | 3992 | 3.252 |
| 16838 | 670.7 | 670.5 | 3993 | 3.252 |
| 66934 | 670.7 | 670.6 | 3994 | 3.252 |

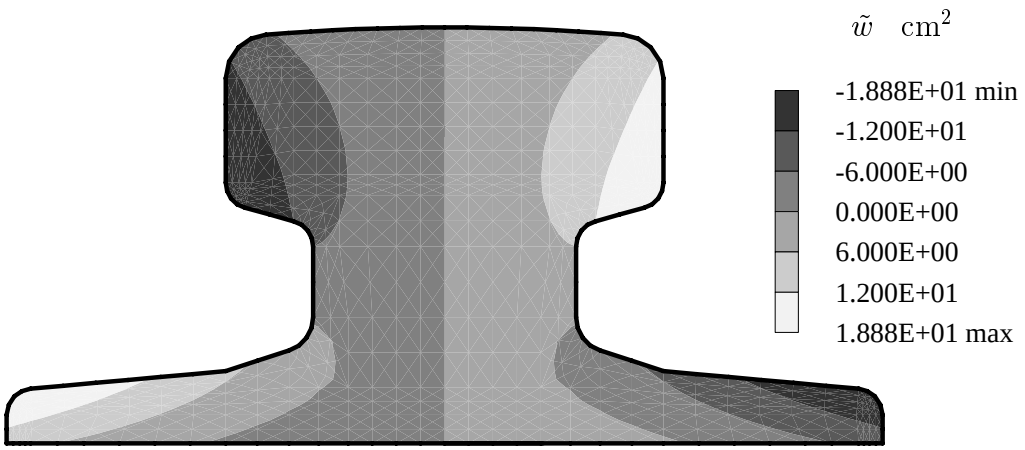


**Figure** 9: Warping function $\tilde{\omega}$ of a crane rail A100

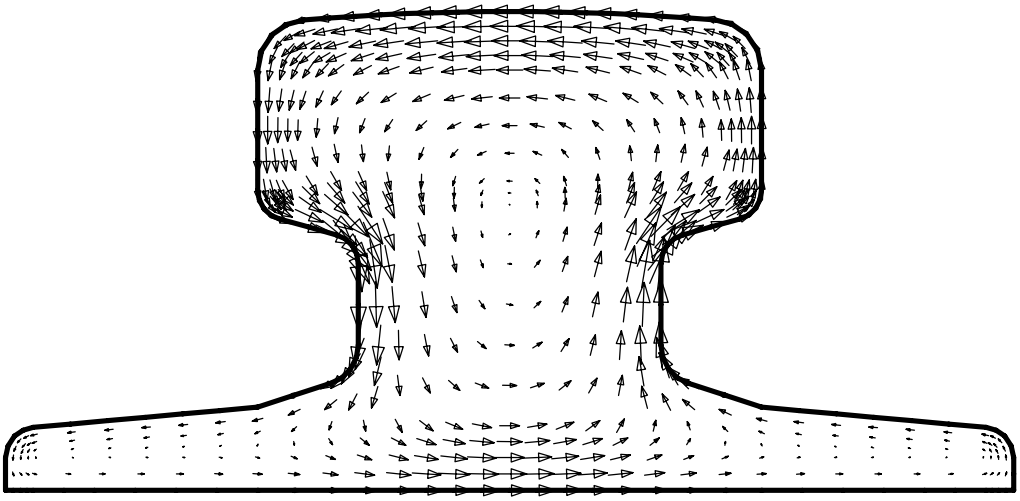

**Figure** 10: Resulting shear stresses of a crane rail A100

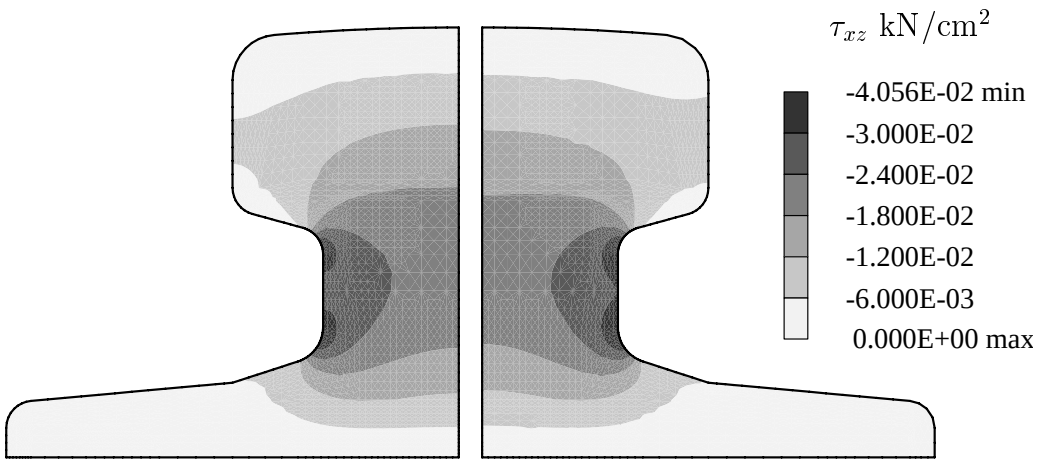


$\nu = 0.0$ $\nu = 0.3$

**Figure** 11: Shear stresses of crane rail A100 for $Q_z = -1\,kN$

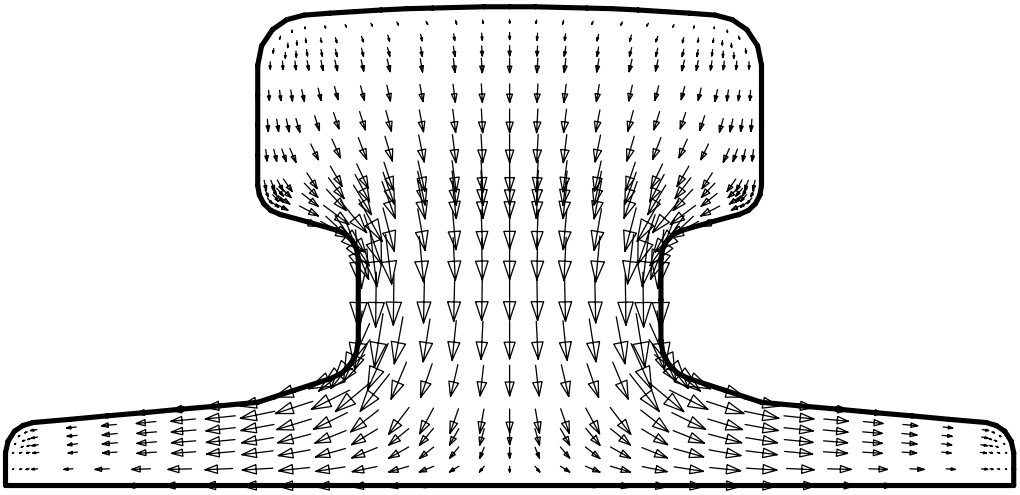

**Figure** 12: Resulting shear stresses of crane rail A100 for $Q_z = -1\,kN$

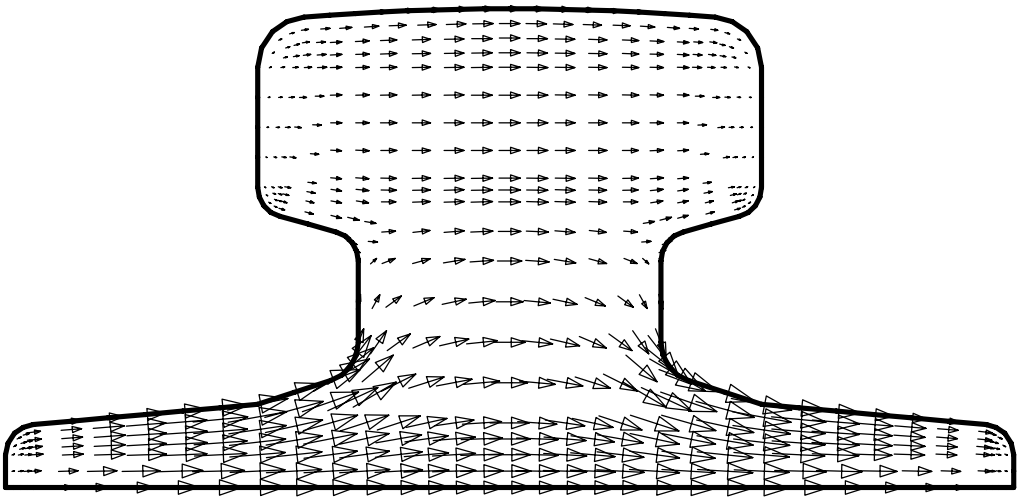

**Figure** 13: Resulting shear stresses of crane rail A100 for $Q_y = 1\,kN$

## 5.4 Bridge cross–section

With the last example we consider a bridge cross–section according to Fig. 14, see [16]. The measurements are given in $m$. Poisson's ratio is taken as $\nu = 0.2$. Considering symmetry the computation can be performed at one half of the cross–section. An adaptive refined mesh for a torsion moment $M_x$ is depicted in Fig. 15. The computed warping and torsion constants are presented in table 4. For comparison in ref. [16] a value $z_M = 1.57\,m$ is given. About 50000 degrees of freedom are necessary for convergence when applying uniform mesh refinement. This confirms the efficiency of adaptive refined meshes. The torsion warping $\tilde{w}$ and the resulting shear stresses are plotted in Figs. 16 and 17, respectively. The torsion stresses act practically only in the closed part of the cross–section. An approximate computation of the torsion stiffness applying Bredt's second formula neglecting the cantilevers yields $I_T = (2A_t)^2 / \oint h^{-1}(s)\,\mathrm{d}s = 40.0\,m^4$.
Next, the constant $z_0$ is evaluated as $z_0 = 1.775\,m$. Finally with $Q_z = 0$ and any value of $\nu$ the coordinate $z_M = 1.569\,m$ is computed using eq. (38). This value corresponds with the coordinate of the center of twist obtained from the warping function, see table 4. The resulting shear stresses are depicted for shear forces $Q_y$ and $Q_z$ in Fig. 18 and Fig. 19, respectively. One can see the qualitative split of the flux at the branches.

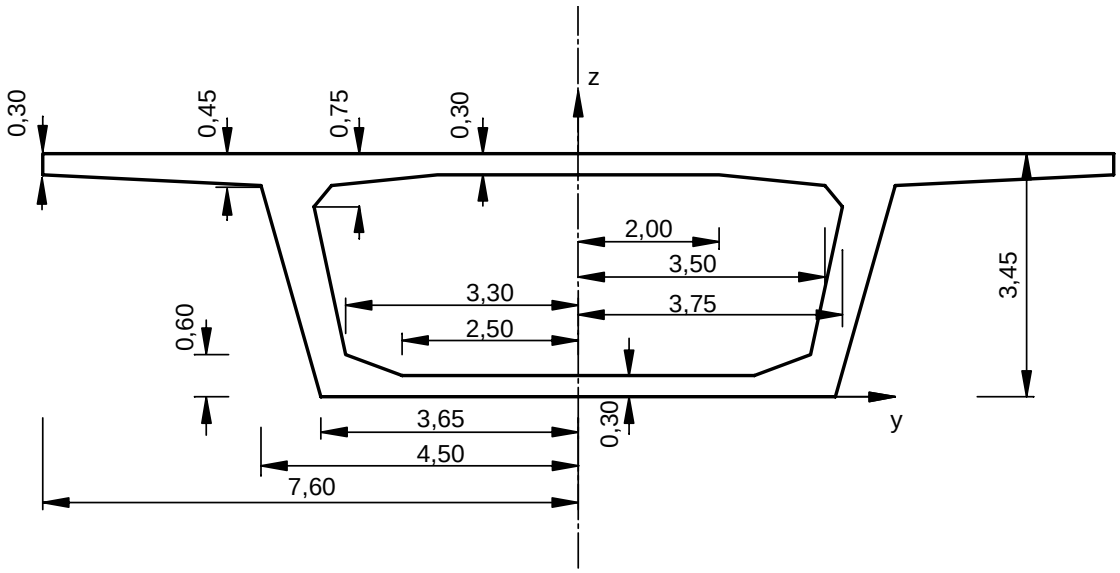


**Figure** 14: Bridge cross–section

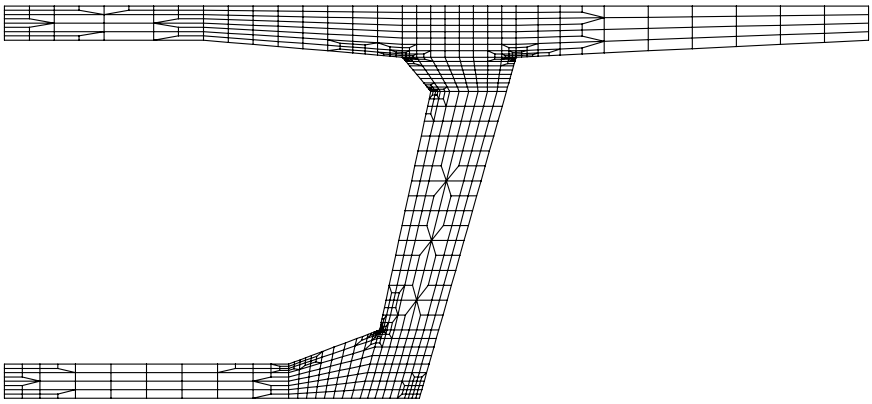

**Figure** 15: Adaptive discretized cross–section

**Table** 4: Torsion and warping properties of the bridge cross–section for adaptive mesh refinement

| $N$ | $I_{T1}$ $m^4$ | $A_{\tilde{\omega}\tilde{\omega}}$ $m^6$ | $z_D$ $m$ |
|---|---|---|---|
| 22 | 43.305 | 65.309 | 1.559 |
| 69 | 42.755 | 63.545 | 1.565 |
| 203 | 42.563 | 63.035 | 1.568 |
| 485 | 42.511 | 62.838 | 1.569 |
| 764 | 42.493 | 62.809 | 1.569 |
| 904 | 42.489 | 62.792 | 1.569 |
| 934 | 42.487 | 62.788 | 1.569 |

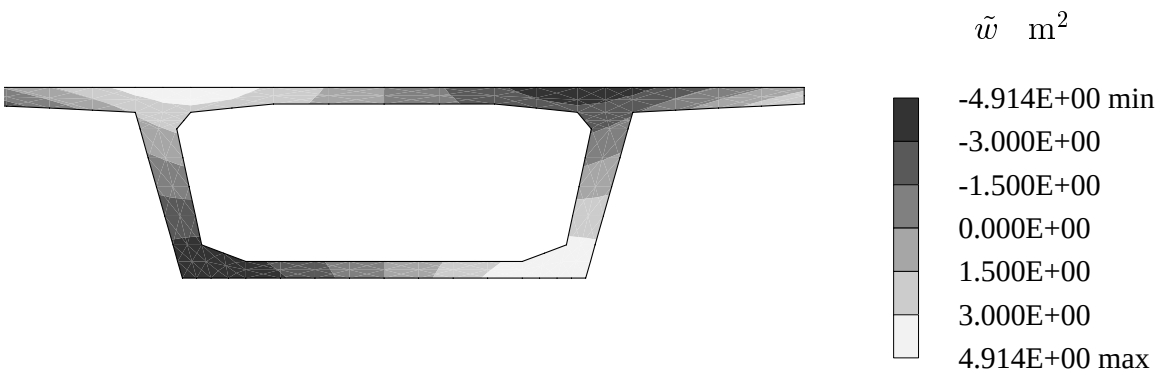


**Figure** 16: Warping function $\tilde{w}$ of the closed cross–section

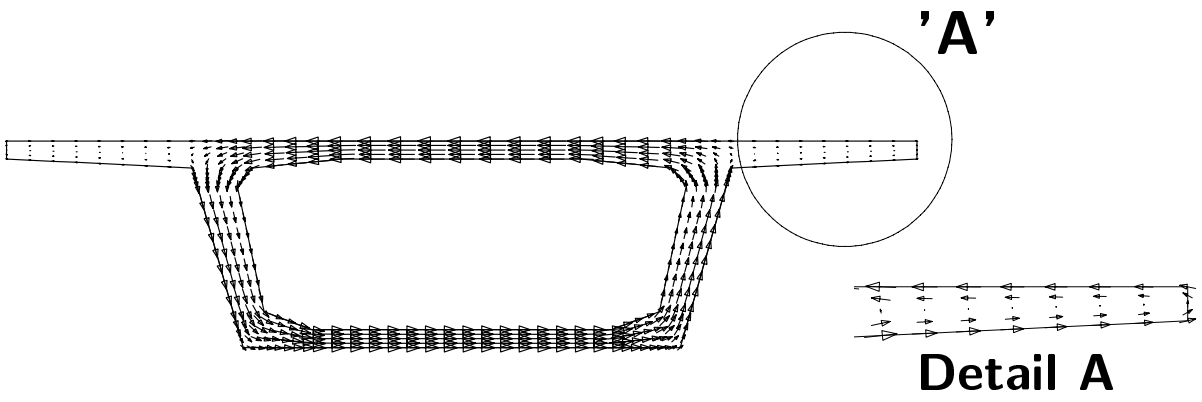


**Figure** 17: Resulting shear stresses for the bridge cross–section under torsion

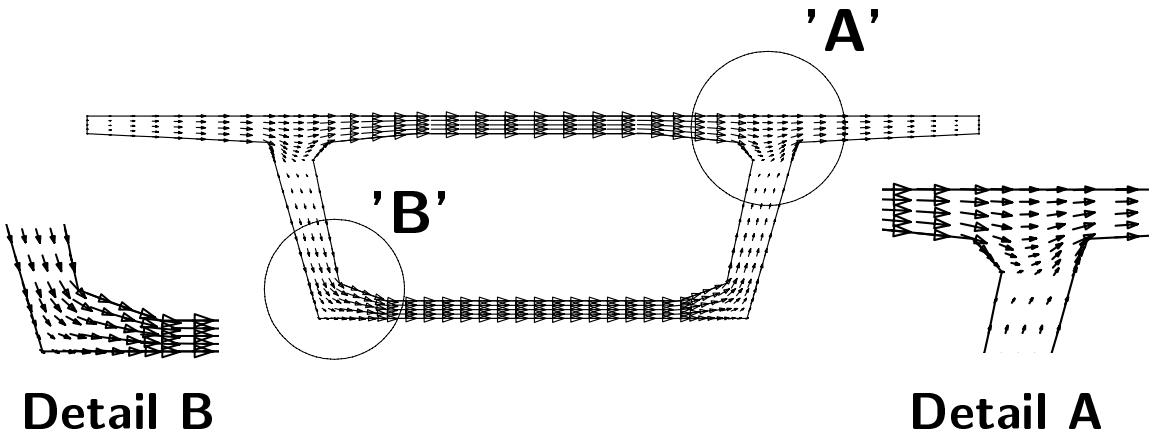


**Figure** 18: Resulting shear stresses of the bridge cross–section for $Q_y = 1\,kN$

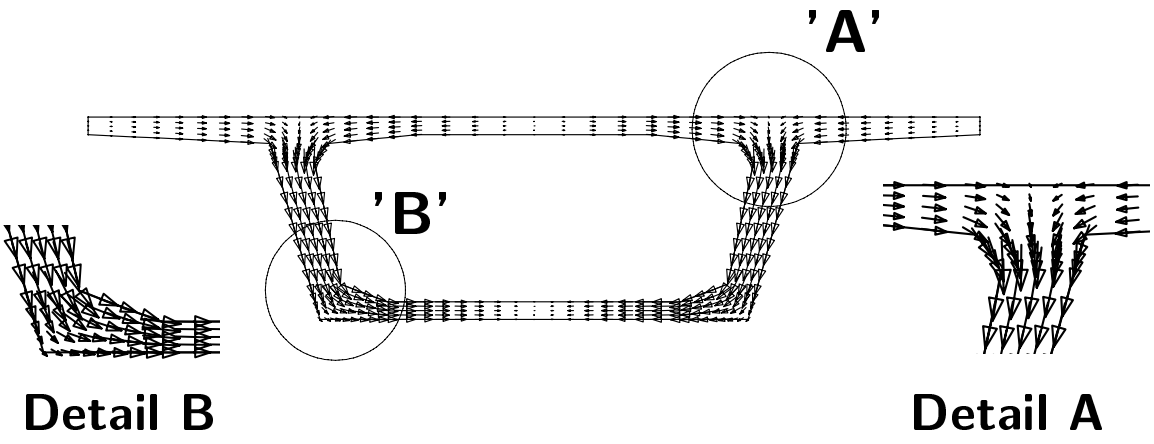


**Figure** 19: Resulting shear stresses of the bridge cross–section for $Q_z = -1\,kN$

# 6 Conclusions

Based on the theory of linear elasticity the shear stresses in prismatic beams subjected to pure torsion and torsionless bending are discussed. For the torsion problem the equilibrium is formulated using the warping function and a stress function. The coordinates of the center of twist, the Saint–Venant torsional stiffness and the warping constant are presented. For the bending problem the equilibrium is fulfilled introducing a stress function. The resulting boundary value problem is derived. The associated Dirichlet boundary conditions are difficult to implement in a finite element program. Therefore, a conjugate stress function is introduced which leads to a Neumann problem. Furthermore, a split into two parts is useful. The integral of the shear stresses of the first part yields the shear force whereas the additional shear stresses of the second part follow from the effect of Poisson's ratio. Within the presented theory it can be shown, that the coordinates of the center of shear and of the center of twist are identical. Based on the derived weak forms of the boundary value problems finite element formulations using isoparametric elements are presented. The discussed examples show the efficiency of adaptive refined meshes in comparison to uniform refined meshes.

# A Appendix

## A.1 Integral of the shear stresses

The integral of the shear stresses $\tau_{xy}$ is reformulated by inserting eqs. $(31)_1$ and $(33)_1$

$$\begin{aligned} \int\limits_{(\Omega)} \tau_{xy}\,\mathrm{d}A &= \int\limits_{(\Omega)} [\bar{\Psi}_{,y} - g_1(z) + \bar{y}(\Delta\bar{\Psi} + f_1)]\,\mathrm{d}A \\ &= \int\limits_{(\Omega)} [(\bar{y}\bar{\Psi}_{,y}\,)_{,y} + (\bar{y}\bar{\Psi}_{,z}\,)_{,z}\,]\,\mathrm{d}A + \int\limits_{(\Omega)} [\bar{y}f_1 - g_1(z)]\,\mathrm{d}A\,. \end{aligned} \tag{66}$$

The first term is integrated by parts and the boundary conditions $(33)_2$ are inserted

$$\begin{aligned} \int\limits_{(\Omega)} \tau_{xy}\,\mathrm{d}A &= \oint\limits_{(\partial\Omega)} \bar{y}(n_y\bar{\Psi}_{,y} + n_z\bar{\Psi}_{,z}\,)\,\mathrm{d}s + \int\limits_{(\Omega)} [\bar{y}f_1 - g_1(z)]\,\mathrm{d}A \\ &= \oint\limits_{(\partial\Omega)} \bar{y}[n_y g_1(z) - n_z g_2(y)]\,\mathrm{d}s + \int\limits_{(\Omega)} [\bar{y}f_1 - g_1(z)]\,\mathrm{d}A\,. \end{aligned} \tag{67}$$

Again integration by parts and considering (22) and (23) leads to

$$\begin{aligned} \int\limits_{(\Omega)} \tau_{xy}\,\mathrm{d}A &= \int\limits_{(\Omega)} [(\bar{y}g_1(z))_{,y} + (-\bar{y}g_2(y))_{,z} + \bar{y}f_1 - g_1(z)]\,\mathrm{d}A \\ &= \int\limits_{(\Omega)} \bar{y}f_1(y,z)\,\mathrm{d}A = a_1 A_{\bar{y}\bar{y}} + a_2 A_{\bar{y}\bar{z}} = Q_y\,. \end{aligned} \tag{68}$$

An analogous derivation can be applied to the integral of $\tau_{xz}$ which yields after some algebra the shear force $Q_z$.

## A.2 Center of shear

The center of shear $M$ is defined as place where the torsion moment in terms of above derived shear stresses vanishes. Considering (38) and $(45)_3$ the coordinates $\{y_M, z_M\}$ follow from the condition

$$Q_z\, y_M - Q_y\, z_M = \int\limits_{(\Omega)} (\tau_{1xz} y - \tau_{1xy} z)\, \mathrm{d}A\,. \tag{69}$$

This equation can be reformulated with above relations. The coordinates $y$ and $z$ are replaced with (10) as $y = -(\Phi_{,y} + \bar{\omega}_{,z})$ and $z = -(\Phi_{,z} - \bar{\omega}_{,y})$. Furthermore, we insert the shear stresses (36) and add the line integrals with the boundary conditions (35), $(9)_2$ with (10).

$$\begin{aligned} Q_z y_M - Q_y z_M &= \int\limits_{(\Omega)} [\bar{\Psi}_{1,y}\,(\Phi_{,z} - \bar{\omega}_{,y}) - \bar{\Psi}_{1,z}\,(\Phi_{,y} + \bar{\omega}_{,z})]\,\mathrm{d}A \\ &= \int\limits_{(\Omega)} (\bar{\Psi}_{1,y}\,\Phi_{,z} - \bar{\Psi}_{1,z}\,\Phi_{,y})\,\mathrm{d}A - \oint\limits_{(\partial\Omega)} (n_y \Phi_{,z} - n_z \Phi_{,y})\,\bar{\Psi}_1\,\mathrm{d}s \\ &\quad - \int\limits_{(\Omega)} (\bar{\Psi}_{1,y}\,\bar{\omega}_{,y} + \bar{\Psi}_{1,z}\,\bar{\omega}_{,z})\,\mathrm{d}A + \oint\limits_{(\partial\Omega)} (n_y \bar{\Psi}_{1,y} + n_z \bar{\Psi}_{1,z})\,\bar{\omega}\,\mathrm{d}s \end{aligned} \tag{70}$$

Hence, application of Green's formula yields

$$Q_z y_M - Q_y z_M = \int\limits_{(\Omega)} (\Phi_{,yz} - \Phi_{,zy})\,\bar{\Psi}_1\,\mathrm{d}A + \int\limits_{(\Omega)} \Delta\bar{\Psi}_1\,\bar{\omega}\,\mathrm{d}A \tag{71}$$

Obviously, the first integral vanishes, whereas the second integral can be rewritten considering the corresponding differential equation in (35)

$$Q_z y_M - Q_y z_M = -\int\limits_{(\Omega)} f_1(y,z)\,\bar{\omega}\,\mathrm{d}A\,. \tag{72}$$

With $Q_y = 0$ one obtains $y_M$ and with $Q_z = 0$ one obtains $z_M$ as

$$y_M = -\frac{A_{\bar{\omega}\bar{z}} A_{\bar{y}\bar{y}} - A_{\bar{\omega}\bar{y}} A_{\bar{y}\bar{z}}}{A_{\bar{y}\bar{y}} A_{\bar{z}\bar{z}} - A_{\bar{y}\bar{z}}^2} \qquad\qquad z_M = \frac{A_{\bar{\omega}\bar{y}} A_{\bar{z}\bar{z}} - A_{\bar{\omega}\bar{z}} A_{\bar{y}\bar{z}}}{A_{\bar{y}\bar{y}} A_{\bar{z}\bar{z}} - A_{\bar{y}\bar{z}}^2}\,. \tag{73}$$

This shows that the coordinates of $M$ can be evaluated with the warping function $\bar{\omega}$ of Saint–Venant's torsion theory. For principal axes the corresponding formulas have been derived by Trefftz [4] using an energy criterion.

# References


[1] C. Weber, 'Biegung und Schub in geraden Balken', *ZAMM* **4**, 334–348 (1924).

[2] C. Weber, 'Übertragung des Drehmoments in Balken mit doppelflanschigem Querschnitt', *ZAMM* **6**, 85–97 (1926).

[3] W. L. Schwalbe, 'Über den Schubmittelpunkt in einem durch eine Einzellast gebogenen Balken', *ZAMM* **15**, 138–143 (1935).

[4] E. Trefftz, 'Über den Schubmittelpunkt in einem durch eine Einzellast gebogenen Balken', *ZAMM* **15**, 220–225 (1935).

[5] J. N. Goodier, 'A theorem on the shearing stress in beams with applications to multicellular sections', *J. Aeronautical Sciences* **11**, 272–280 (1944).

[6] W. R. Osgood, 'The center of shear again', *J. Appl. Mech.* **10**(2), A-62–A-64 (1943).

[7] A. Weinstein, 'The center of shear and the center of twist', *Quart. of Appl. Math.* **5**(1), 97–99 (1947).

[8] E. Reissner and W. T. Tsai, 'On the determination of the centers of twist and of shear for cylindrical shell beams', *J. Appl. Mechanics* **39** 1098–1102 (1972).

[9] S. P. Timoshenko and J. N. Goodier, *Theory of Elasticity*, 3rd edn, McGraw–Hill International Book Company, 1984.

[10] I. S. Sokolnikoff, *Mathematical Theory of Elasticity*, McGraw–Hill, New York, 1956.

[11] W. E. Mason and L. R. Herrmann, 'Elastic shear analysis of general prismatic beams', *J. Eng. Mech. Div.* ASCE **94**, EM4, 965–983 (1968).

[12] L. R. Herrmann, 'Elastic torsional analysis of irregular shapes', *J. Eng. Mech. Div.* ASCE **91**, EM6, 11–19 (1965).

[13] J. L. Krahula and G. L. Lauterbach, 'A finite element solution for Saint–Venant Torsion', *AIAA Journal* **7**(12), 2200–2203 (1969).

[14] G. Haberl and F. Och, 'Eine Finite–Element–Lösung für die Torsionssteifigkeit und den Schubmittelpunkt beliebiger Querschnitte', *Z. f. Flugwiss.* **22**(4), 115–119 (1974).

[15] C. Zeller, 'Querschnittsverformungen von Stäben', *Ingenieur–Archiv* **52**, 17–37 (1982).

[16] C. Zeller, 'Zur Bestimmung der Verwölbungen und Profilverformungen von elastischen Stäben mit beliebigen und dünnwandigen Querschnitten', *Ingenieur–Archiv* **55**, 376–387 (1985).

[17] F. W. Bornscheuer, 'Systematische Darstellung des Biege– und Verdrehvorgangs unter besonderer Berücksichtigung der Wölbkrafttorsion', *Der Stahlbau* **21**(1), 1–9 (1952).

[18] F. Gruttmann, W. Wagner and R. Sauer, 'Zur Berechnung von Wölbfunktion und Torsionskennwerten beliebiger Stabquerschnitte mit der Methode der finiten Elemente', *Bauingenieur* **73**(3), 138–143 (1998).

[19] O. C. Zienkiewicz and J. Z. Zhu, 'A simple error estimator and adaptive procedure for practical engineering analysis', *Int. J. Num. Meth. Engng.* **24**, 337–357 (1987).

[20] O. C. Zienkiewicz and R. L. Taylor, *The Finite Element Method*, 4th edn, McGraw–Hill, London, 1989.